Chaos, Solitons and Fractals 172 (2023) 113547

Contents lists available at ScienceDirect

Chaos, Solitons and Fractals

journal homepage: www.elsevier.com/locate/chaos

Dynamical and topological conditions triggering the spontaneous activation of Izhikevich neuronal networks

Sergio Faci-Lázaro [a,b], Jordi Soriano [c,d], Juan José Mazo [e], Jesús Gómez-Gardeñes [a,b,*]

[a] Departmento de Física de la Materia Condensada, Universidad de Zaragoza, 50009 Zaragoza, Spain
[b] GOTHAM Lab – Institute for Biocomputation and Physics of Complex Systems (BIFI), University of Zaragoza, 50018 Zaragoza, Spain
[c] Departament de Física de la Matèria Condensada, Universitat de Barcelona, Barcelona 08028, Spain
[d] Universitat de Barcelona Institute of Complex Systems (UBICS), 08028 Barcelona, Spain
[e] Departamento de Estructura de la Materia, Física Térmica y Electrónica and Grupo Interdisciplinar de Sistemas Complejos (GISC), Universidad Complutense de Madrid, 28040 Madrid, Spain

ARTICLE INFO

Keywords:
Complex networks
Izhikevich model
Master Stability Function

ABSTRACT

Understanding the dynamic behavior of neuronal networks *in silico* is crucial for tackling the analysis of their biological counterparts and making accurate predictions. Of particular importance is determining the structural and dynamical conditions necessary for a neuronal network to activate spontaneously, transitioning from a quiescent ensemble of neurons to a network-wide coherent burst. Drawing from the versatility of the Master Stability Function, we have applied this formalism to a system of coupled neurons described by the Izhikevich model to derive the required conditions for activation. These conditions are expressed as a critical effective coupling g_C, grounded in both topology and dynamics, above which the neuronal network will activate. For regular spiking neurons, average connectivity and noise play a significant role in their ability to activate. We have tested these conditions against numerical simulations of *in silico* networks, including both synthetic topologies and a biologically-realistic spatial network, showing that the theoretical conditions are well satisfied. Our findings indicate that neuronal networks readily meet the criteria for spontaneous activation, and that this capacity is weakly dependent on the microscopic details of the network as long as average connectivity and noise are sufficiently strong.

1. Introduction

Understanding the relationship between the structure and function of neuronal networks is a fundamental goal of modern neuroscience. To address this complex problem, researchers have combined insights from various disciplines, from physiology and imaging techniques to nonlinear and statistical physics tools [1,2].

A successful approach to studying neuronal networks involves combining experimental data from biological neuronal cultures with theoretical modeling and numerical simulations. Cultures provide a simplified yet living system in which the neuronal network's entire population can be monitored and perturbed at both the neuronal and connectivity levels [3–6]. Meanwhile, theoretical and numerical approaches utilize experimental data to create *in silico* replicas of biological networks. This allows researchers to identify the most important building blocks that govern network behavior and formulate predictions [7–9].

Thanks to the above multidisciplinary approach, the mechanisms underlying collective behavior in neuronal networks, e.g. spontaneous activity or synchronization, are being brought to light. Central mechanisms include metric correlations inherited from the spatial embedding of these networks [10–15], noise [16], and high-order organizational traits such as modularity [17]. Altogether, these mechanisms are sufficient to drive robust, nearly periodic episodes of collective spontaneous activity whose spatiotemporal richness is highly tied to the underpinned structural connectivity that dictates the interaction between neurons.

Numerical models of living neuronal networks are important not only to shape biologically-realistic networks and mimic their spatial constraints [7], but also to compare the possible benefits and drawbacks of synthetic configurations, e.g., random geometric graphs or well-known topologies such as the Erdös–Rényi, Barabàsi–Albert or Watts–Strogatz network models. By comparing the behavior of biologically-realistic networks with these models one can investigate the importance of spatial constraints in shaping key topological features and molding collective behavior [18].

* Corresponding author at: Departmento de Física de la Materia Condensada, Universidad de Zaragoza, 50009 Zaragoza, Spain.
E-mail address: gardenes@unizar.es (J. Gómez-Gardeñes).

https://doi.org/10.1016/j.chaos.2023.113547
Received 10 March 2023; Received in revised form 4 May 2023; Accepted 7 May 2023
Available online 20 May 2023

There are many models able to capture the intrinsic nonlinear nature of neurons, from the highly accurate Hodgkin–Huxley and its simplified Fitzhugh–Nagumo version to the highly-efficient quadratic integrate-and- fire and Izhikevich models [19–23]. However, despite the success of several studies in building suitable neuron network models, an aspect that is still poorly explored is the interrelation between the dynamical model describing the neurons and the connectivity established between neurons.

To explore this aspect, the present work investigates the relationship between the dynamics of the simulated neurons and the connectivity of the network they are embedded in. Such a relationship is conceived by deriving the Master Stability Functions (MSFs) and Conditions (MSCs) of such a dynamical system [24–26], thus providing general insights on the dynamical behavior of the neuronal networks under study [27–29]. The dynamical system that we analyze is the celebrated Izhikevich model [21,22], which is able to capture several neuronal types and behaviors while maintaining mathematical simplicity and computational efficiency [30]. Thus, here we unveiled the fundamental relationships that govern the interplay between the connectivity layout among neurons, their coupling strength, and noise, to later predict the spectrum of activity regimes that the network can exhibit.

The article is structured as follows. In Section 2 we first analyze the Izhikevich model, one of the most widely used models to describe the behavior of *in silico* neuronal cultures [30]. In Section 3 we derive the Master Stability Function and Condition for the stability of the stationary state, and predict the critical value of the coupling between neurons at which the stability of the quiescent state is lost. Finally, in Sections 4 and 5 we test our results using realistic models for both neuronal dynamics and structural connectivity.

2. Izhikevich model

We start by describing in detail the dynamical network model used in this work. In particular, we consider a network of N neurons whose dynamics was described by the Izhikevich model [21,22]. In particular, the dynamical evolution of a node, say i, of the network is given by:

$$\begin{aligned} \dot{x}_i &= a(x_i - x^r)(x_i - x^t) - y_i + \xi_i + I_i, \\ \dot{y}_i &= b(x_i - x^r) - y_i, \\ x_i \geqslant p \longrightarrow & \begin{cases} x_i \longleftarrow c, \\ y_i \longleftarrow y_i + d, \end{cases} \end{aligned} \tag{1}$$

where x_i and y_i are the membrane potential and inhibitory current, respectively, of a neuron i in the network, and x^r and x^t are the resting and threshold potentials (being $x^r < x^t$). The parameters a and b account for the sensitivity to subthreshold fluctuations, c and d regulate the reset conditions after the neuron has fired an action potential (spike), and ξ_i and I_i account, respectively, for the inputs that neuron i receives as noise from the environment and the input currents that reach it through its synapses.

The term I_i is particularly important since it depends on the arrival of inputs from other neurons in the network, and is described as a time-independent step function:

$$I_i = g \sum_{j=1}^{N} A_{ji} \Theta(x_j - x^t), \tag{2}$$

where g is the strength of each synaptic input. Conceptually, g describes the coupling between neurons in the network, analytically captured by the adjacency matrix $\boldsymbol{A}$, which is assumed for simplicity to be symmetric ($A_{ij} = A_{ji}$) and unweighted, i.e., $A_{ij} = 1$ if there is a connection between neurons i and j, and 0 otherwise.

The noise term ξ_i in Eq. (1) is also important for it reflects the noisy nature of biological systems. Following Ref. [7], we implemented two sources of noise. The first source represents the fluctuations in neuronal afferents (input connections) and that is modeled as a positive half-Gaussian white noise, centered at 0 and with variance g_W^2. The second source accounts for the spontaneous release of neurotransmitters in presynaptic terminals, which induce small currents on the postsynaptic neuron and that occur independently of whether the postsynaptic neuron is active or not [31,32]. These small currents are usually called *minis* and can be mathematically described as shots of characteristic frequency λ and strength g_S.

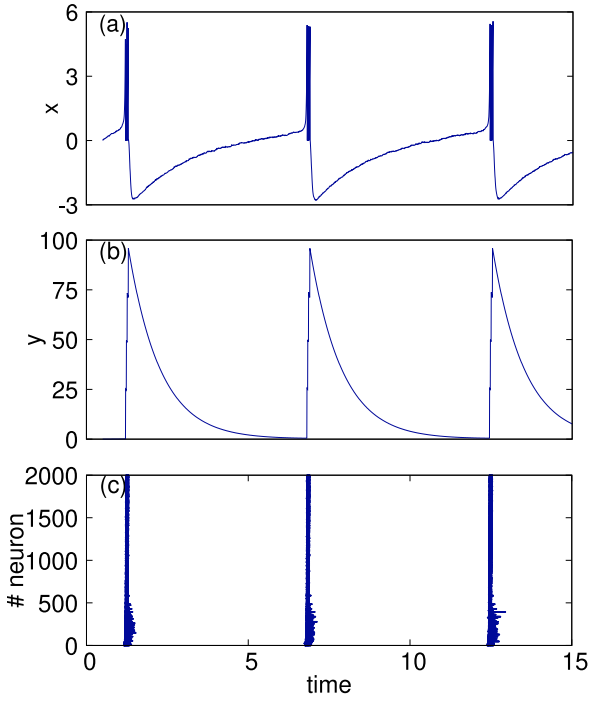

Fig. 1. Dynamical behavior of the Izhikevich neuron model. (a) Evolution of the membrane potential with time, $x_i(t)$. (b) Evolution of the inhibitory current with time, $y_i(t)$. (c) Network collective activity visualized as a raster plot. For this simulation, an Erdös–Rényi network of $N = 2,000$ and $\langle k \rangle = 25$. In addition, the values of the parameter of the Izhikevich model are $a = 7.5$, $b = 0.5$, $c = 0$, $d = 3.5$, $p = 6$ as well as $x^r = 0$ and $x^t = 1$ for the rest and threshold values and $g = 2$, $g_W = 2$, $g_S = 0.2$, $\lambda = 0.5$ for the current values.

Fig. 1(a)–(b) provides an example of the dynamics of a single Izhikevich neuron, characterized by the spiking behavior of the membrane potential x [Fig. 1(a)] and the fast activation of the inhibitory current y as soon as the neuron has fired [Fig. 1(b)]. Let us note that the capacity of the neuron to activate is tightly linked to the values of the resting x^r and threshold x^t potentials. Indeed, the membrane potential will remain around its resting value when the number of external inputs is insufficient to reach the threshold. However, as soon the inputs suffice to pass the threshold the neuron will activate and transmit an electric pulse to its downstream postsynaptic neighbors. At this point, neuron's membrane potential x_i will grow up to a peak value p. Then, the membrane potential as well as the inhibitory currents will be reset to $x_i = c$ (with $c < x^t$) and $y_i = y_i + d$, and the neuron will gradually return to its inactive state.

The coupling of neurons through a network leads to collective behavior whose structure depends on the connectivity among neurons. In a typical scenario in which neuronal connectivity is similar and large enough across the network, network dynamics is characterized by synchronous activity patterns in which all neurons activate during a short time window (network bursts) and remain quiescent in between bursts [7,16]. This coherent dynamical is illustrated in Fig. 1(c).

It should be noted that, to favor mathematical analysis, the model can be scaled (without loss of generality) by setting the resting and threshold potentials as $x^r = 0$ and $x^t = 1$. Additionally, time t as well as all other variables and parameters can be set dimensionless.

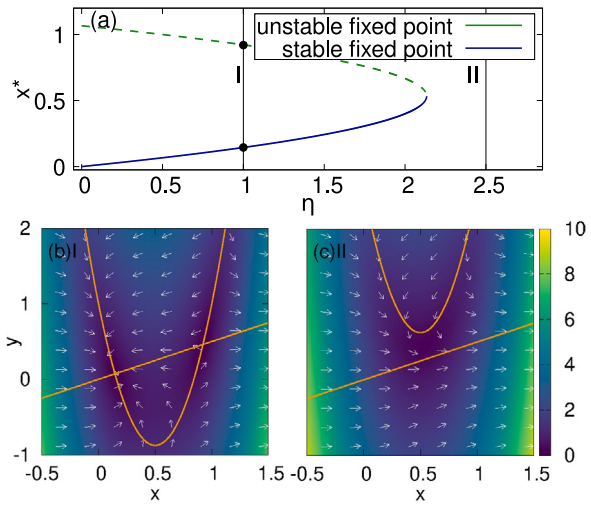

Fig. 2. Analysis of stability. (a) Representation of the solutions $x^*_\pm$ and $y^*_\pm$, since $y^*_\pm = b \cdot x^*_\pm$, from Eq. (3) as a function of the external input η. No fixed points exist above the saddle-node bifurcation, for $\eta \geqslant \eta_C \approx 2.13$. (b) and (c) correspond to the flux maps of the dynamical system for different values of η (1.0 and 2.5). Orange lines and curves are the nullclines. The color scale and arrows represent the module and direction of the velocities in each point. (For interpretation of the references to color in this figure legend, the reader is referred to the web version of this article.)

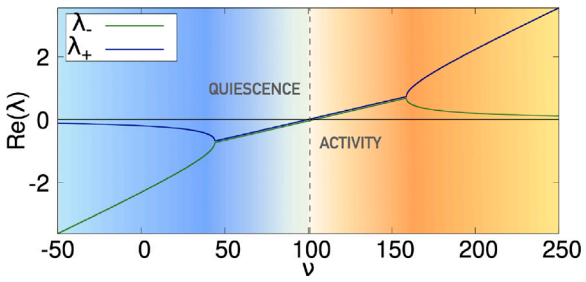

Fig. 3. Evolution of the eigenvalues $\lambda_\pm$ as a function of the effective coupling ν for an average input noise of $\eta = 2.0$. The stable solutions to the master stability function are $\mathrm{Re}(\lambda_+) \geqslant \mathrm{Re}(\lambda_-)$, and thus $\mathrm{Re}(\lambda_+)$. The value of ν_{MAX} corresponds to the intersection of $\mathrm{Re}(\lambda_+) = 0$, shown with the orange line. Any other value of ν above it will take the system out of the stable quiescent state into the active state. (For interpretation of the references to color in this figure legend, the reader is referred to the web version of this article.)

3. Derivation of the Master Stability Function

In order to derive a Master Stability Function, we first focus on the behavior of a single neuron as a function of the external input $\eta = \xi + I$, to study the existence and stability of the stable solutions of the model. To this aim, we compute the fixed points as the intersection between the nullclines $\dot{x} = 0$ and $\dot{y} = 0$ in Eq. (1) obtaining, for all $\eta \leqslant \eta_C = (a+b)^2/4a$,

$$\begin{aligned} x^*_\pm &= \left(\tfrac{a+b}{2a}\right)\left(1 \pm \sqrt{1 - \tfrac{\eta}{\eta_C}}\right) \\ y^*_\pm &= b x^*_\pm \end{aligned} \quad . \tag{3}$$

As shown in Fig. 2(a) the dynamical system experiences a saddle-node bifurcation at a critical value $\eta = \eta_C$. For $\eta < \eta_C$ there exist two fixed points, a stable one corresponding to the negative branch, (x^*_-, y^*_-), and an unstable one corresponding to the positive branch, (x^*_+, y^*_+). As η increases and approaches η_C from below these points becomes closer. At $\eta = \eta_C$, the system undergoes a saddle-node bifurcation, i.e., the two fixed points coalesce into a half-stable fixed point that vanishes as soon as $\eta > \eta_C$.

Considering the former bifurcation for a single neuron it is clear that, in order to be able to study the stability of a stationary state of an ensemble of coupled neurons, we need an average input η smaller than the threshold η_C. Hence, assuming that this condition is satisfied, we can advance a step forward and derive the MSF of a networked system of neurons whose interaction backbone is given by an adjacency matrix, $\boldsymbol{A}$.

3.1. Derivation of the critical coupling

As usual in the derivation of the MSF of a networked system of coupled dynamical units [25,26], we start by carrying a linear stability analysis of the solution of interest that, in our case, is the fixed point (x^*_-, y^*_-). Taking into account that all the neurons in the system have identical states, *i.e.* $(x^*_i, y^*_i) = (x^*_-, y^*_-)\ \forall i = 1, \ldots, N$, we explore the behavior of the system under a small enough perturbations. Thus, we will assume the system is in the perturbed state $(x_i, y_i) = (x^*_-, y^*_-) + (\epsilon^x_i, \epsilon^y_i)$, with $|\epsilon^x_i / x^*_-| \ll 1$ and $|\epsilon^y_i / y^*_-| \ll 1\ \forall i = 1, \ldots, N$.

To obtain the evolution of the perturbations $(\epsilon^x_i, \epsilon^y_i)$ we make use of a Taylor expansion of the system described in Eqs. (1) and (2) around the fixed point solution. Identifying the functions describing the local dynamics in Eq. (1) as $f^x(x,y) = ax(x-1) - y + \eta$ and $f^y(x,y) = bx - y$; and the ones describing the interaction dynamics as $g^x(x) = g\Theta(x-1)$ and $g^y = 0$, we arrive at:

$$\begin{aligned} \dot{\boldsymbol{\epsilon}}^x &= \left(a^{xx}\mathbf{I} + c^{xx}\boldsymbol{A}^T\right)\boldsymbol{\epsilon}^x + a^{xy}\boldsymbol{\epsilon}^y, \\ \dot{\boldsymbol{\epsilon}}^y &= a^{yx}\boldsymbol{\epsilon}^x + a^{yy}\boldsymbol{\epsilon}^y, \end{aligned} \tag{4}$$

where $a^{\alpha\beta}$ and $c^{\alpha\beta}$ for $\alpha, \beta = x, y$ are defined as:

$$a^{\alpha\beta} := \left.\frac{\partial f^\alpha}{\partial \beta}\right|_{(x^*_-, y^*_-)}, \quad c^{\alpha\beta} := \left.\frac{\partial g^\alpha}{\partial \beta}\right|_{(x^*_-, y^*_-)}, \tag{5}$$

With the former definitions, Eq. (4) can be written in a compact manner as:

$$\dot{\boldsymbol{\epsilon}}^\alpha = \sum_{\beta=x,y} \left(a^{\alpha\beta}\mathbf{I} + c^{\alpha\beta}\boldsymbol{A}^T\right)\boldsymbol{\epsilon}^\beta. \tag{6}$$

Now, assuming that the transpose of the adjacency matrix has N distinct eigenvectors, $\boldsymbol{w}_n$, with eigenvalues, λ_n, $\forall n = 1, \ldots, N$, we can expand the vector $\boldsymbol{\epsilon}^\alpha(t)$ as a linear combination of the elements of this basis with components $\boldsymbol{\chi}^\alpha(t)$:

$$\boldsymbol{\epsilon}^\alpha(t) = \boldsymbol{W}^T \boldsymbol{\chi}^\alpha(t). \tag{7}$$

Thus, in the new basis, Eq. (6) reads:

$$\dot{\boldsymbol{\chi}}^\alpha = \sum_{\beta=x,y} \left(a^{\alpha\beta}\mathbf{I} + c^{\alpha\beta}\boldsymbol{\Lambda}\right)\boldsymbol{\chi}^\beta. \tag{8}$$

This equation shows that the dynamics of the neuronal network are (locally) asymptotically stable near the equilibrium (x^*_-, y^*_-) if and only if all real parts of the eigenvalues of the matrix $\boldsymbol{M}(\lambda) = [a^{\alpha\beta} + \lambda c^{\alpha\beta}]$ are negative, denoted as $\mathrm{Re}(\lambda_\pm) < 0\ \forall n = 1, \ldots, N$, especially the larger one. Thus, by substituting the expressions of $a^{\alpha\beta}$ and $c^{\alpha\beta}$ into $\boldsymbol{M}$, we derive the following equation:

$$\boldsymbol{M} = \begin{pmatrix} a(2x^*_- - 1) & -1 \\ b & -1 \end{pmatrix} + \lambda g \begin{pmatrix} \Gamma(x^*_-) & 0 \\ 0 & 0 \end{pmatrix}, \tag{9}$$

where $\Gamma(x^*_-) = \left.\frac{d}{dx}\Theta(x-1)\right|_{x^*_-}$. Finally, by introducing the effective coupling, given by $\nu := \lambda g$, and computing the eigenvalues of $\boldsymbol{M}$ we obtain:

$$\begin{aligned} \lambda_\pm &= \tfrac{1}{2}\left[(Q-1) \pm \sqrt{(Q+1)^2 - 4b}\right], \\ Q &:= a(2x^*_- - 1) + \nu\Gamma(x^*_-). \end{aligned} \tag{10}$$

We note that the interesting eigenvalue is λ_+, since $\mathrm{Re}(\lambda_+) \geqslant \mathrm{Re}(\lambda_-)$ $\forall \nu$, and thus the function $\mathrm{Re}(\lambda_+)(\nu)$ is our MSF.

From Eq. (10) we can analyze the shape of $\lambda_\pm$ as a function of the effective coupling ν. As shown in Fig. 3, there exists a maximum value of the effective coupling, ν_{MAX}, above which the system loses stability

and becomes active. Taking into account that $\lambda_+(\nu_{MAX}) = 0$, we can obtain the effective coupling threshold as:

$$\nu_{MAX} = \lambda_{MAX} \cdot g_C = \frac{b - a(2x^*_- - 1)}{\Gamma(x^*_-)}. \tag{11}$$

The former equation allow us to provide the stability condition for a given network of coupled neurons. In particular, given an adjacency matrix with maximum eigenvalue λ_{MAX} and considering the estimation $\lambda_{MAX} \approx \frac{\langle k^2 \rangle}{\langle k \rangle}$ [33,34], we can finally derive the critical value of the coupling strength g_C above which the system becomes active as:

$$g_C = \frac{\langle k \rangle}{\langle k^2 \rangle} \frac{b - a(2x^*_- - 1)}{\Gamma(x^*_-)}. \tag{12}$$

It is important to note that the value of g_C only depends on the intrinsic parameters of the model, a and b, the average level of inputs that each node receives, η, which determines the fixed point, and the connectivity structure of the system.

Finally, it is worth mentioning that, for analytical purposes, the coupling function $g(x)$ in Eq. (2) must be continuous and differentiable. For this reason, we approximated the step function Θ to $\Theta(x - 1) \approx \frac{1}{2}\{1 + \tanh[\gamma(x - 1)]\}$. By doing so, a new parameter, γ, is added to the model. This parameter is related to the steepness of the coupling function, providing a measure of how much influence a neuron has over its neighbors when its membrane potential is around the activation threshold. This way, by tuning this parameter, our model can be adjusted so that the effective synaptic current the neurons receive is the same as when implementing more complex coupling functions [22,23]. It is important to note however, that even if the value of γ has to be tuned, it is independent from any other parameter, structural or dynamical, of the model.

4. Advanced Izhikevich model

To further explore the relation between network activation and its underlying topological and dynamical traits, we now consider a refinement of the Izhikevich model to be more biologically accurate. In particular, we aim at incorporating synaptic depression, i.e., the gradual decay in synaptic efficiency as neurons elicit spikes. Such a refinement was successfully introduced in Refs. [7,8] to mimic biological neurons *in silico* and, while the equations describing the dynamics of the *soma* are the same as the ones introduced in Eq. (1), those capturing the dynamics of synapses (initially described in Eq. (2)) now take the following form:

$$\begin{aligned} I_j(t) &= \sum_{i=1}^{N} \sum_{t_m < t} A_{ij} E_i(t, t_m), \\ E_i(t, t_m) &= g_A D_i(t_m) \exp\left(-\tfrac{t - t_m}{\tau_A}\right) \Theta(t - t_m), \\ \dot{D}_i &= \tfrac{1 - D_i}{\tau_D} - (1 - \beta) D_i \delta(t - t_m), \end{aligned} \tag{13}$$

where $E_i(t, t_m)$ is the current induced by the i−th neuron at a time t as a result of the spike generated at time t_m. The parameters g and τ_A correspond to the strength and decay time of the synaptic current, respectively. $D_i(t)$ is the depression term that describes the efficacy of the neuron's presynaptic terminals. It has a resting value of 1 and relaxes exponentially with a decay time of τ_D. Finally, β is a coefficient related to the loss in efficiency that occurs whenever a synaptic pulse is generated.

This detailed Izhikevich model can be numerically explored by conducting simulations in synthetic networks. In particular, we can check the validity of the critical value of the coupling strength g_C derived by the MSF, Eq. (12), by comparing with the numerical results obtained for g_C in the advanced Izhikevich model described above. To do so we consider two of the most paradigmatic models of coupling networks, Erdös-Rényi (ER) graphs [35,36] and Barabási–Albert scale-free (BA) networks [37], and compute the theoretical and numerical values of g_C when changing the average connectivity $\langle k \rangle$ in both models.

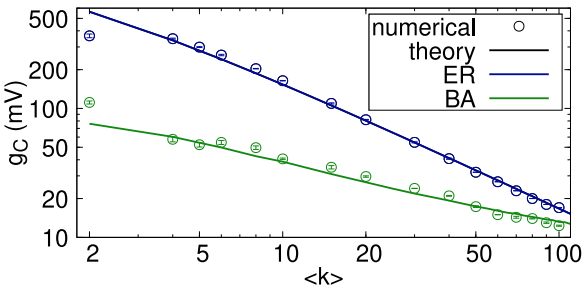

Fig. 4. Dependence of the critical coupling g_C on the average connectivity $\langle k \rangle$ for ER and BA networks of $N = 2000$ nodes. The dots correspond to numerical simulations of ER and BA networks with an Izhikevich model that incorporates depression whereas the solid lines corresponds to the theoretical predictions of g_C given by Eq. (12). The theoretical predictions for ER and BA have been obtained with $\gamma_{ER} = 4.7$ and $\gamma_{BA} = 5.1$ respectively. Numerical simulations were averaged over $n = 25$ network realizations. Error bars indicate standard deviation.

As shown in Fig. 4, despite of the approximations made to the Izhikevich model to derive the MSF (and g_C), the numerical integration (open circles) of the refined model follows the same theoretical trend predicted by MSF, thus pinpointing that depression does not play an important role in the activation of a neuronal network. Besides, the trend $g_C \sim \langle k \rangle^{-1}$ observed in Fig. 4 for homogeneous networks can be easily recovered from Eq. (12) considering that for ER graphs $\langle k^2 \rangle = \langle k \rangle(1 + \langle k \rangle)$.

It is worth to remark that the γ parameter used to obtain the theoretical predictions does not depend of $\langle k \rangle$, i.e. it is the same for the whole set of networks generated by each model. Moreover, the resulting values after the calibration with numerical results are quite similar for both models, being $\gamma_{ER} = 4.7$ and $\gamma_{BA} = 5.1$.

5. Stability in biologically-realistic networks

So far, we have explored the dependence of the critical coupling g_C on connectivity in simple synthetic topologies, where the first and second moments of the degree distribution are essentially linked to the probability of any two neurons in the network to connect. However, since the Izhikevich model is mainly implemented to describe the dynamic behavior of biologically-realistic neurons, it is also important to study the accuracy of our theoretical predictions when the connectivity layout incorporates biological traits, most notably spatial embedding, anistropies, and distance-dependent connectivity.

To achieve this biologically-realistic connectivity, we implemented the structural model developed in [7,8]. As sketched in Fig. 5(a), a neuron is modeled with the following characteristics:

- Its cell body (soma) is circular with a fixed diameter ϕ_s.
- Its dendritic trees is also circular with the soma at its center. The diameter of the dendritic tree ϕ_d is drawn from a Gaussian distribution with an average of μ_d and a standard deviation of σ_d:

$$p(\phi_d) = \frac{1}{\sqrt{2\pi\sigma_d^2}} \exp\left[-\frac{(\phi_d - \mu_d)^2}{2\sigma_d^2}\right]. \tag{14}$$

- The axon of the neuron has a length ℓ given by a Rayleigh distribution with a standard deviation σ_ℓ:

$$p(\ell) = \frac{\ell}{\sigma_\ell^2} \exp\left(-\frac{\ell^2}{2\sigma_\ell^2}\right). \tag{15}$$

The maximum axonal length allowed in the network is ℓ_{MAX} in order to control the amount of long range connections in the synthetic culture. In addition, the axon is modeled as a concatenation of segments of fixed length $\Delta\ell$. The first segment is placed at

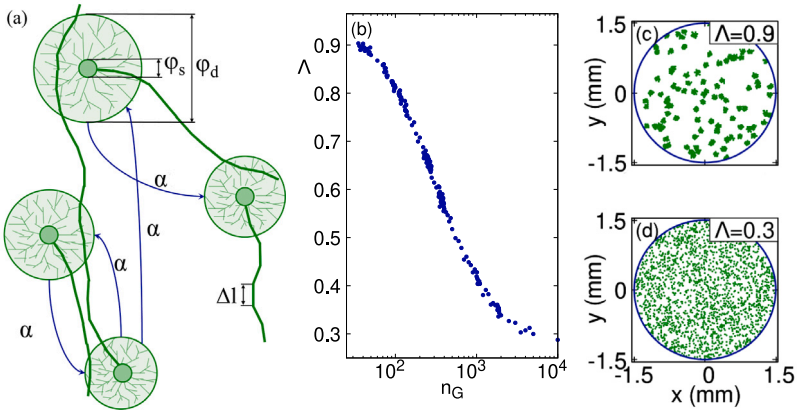

Fig. 5. (a) Schematic representation of a neuron as well as the process of building the connections in a neuronal network according to a spatial model. In the figure a few neurons are shown connected with each other. Each neuron is composed of a *soma* with diameter ϕ_s, a dendritic tree modeled as a circle of diameter ϕ_d and an axon of length ℓ built as a concatenation of segments, each with a length of $\Delta\ell$. The blue arrows represent the potential synaptic connection between these neurons. These potential connections correspond to all the intersections between dendritic trees and axons of different neurons, and will take place with a connection probability α. (b) Evolution of the aggregation coefficient, Λ, as a function of the number of Gaussian centers n_G used to built the spatial probability. As expected, the degree of aggregation of the networks decreases with the number of Gaussian center used to build the spatial probability distribution of neurons. It is important to notice that, despite our best efforts, a perfectly homogeneous ($\lambda = 0$) or a perfectly aggregated ($\Lambda = 1$) networks are no computationally feasible (if not impossible) with this model. (c) and (d) show examples of the spatial distribution of the somas for aggregated ($\Lambda = 0.9$ or $n_G = 50$) and quasi-homogeneous ($\Lambda = 0.3$ or $n_G = 5,000$) networks. Green dots represent the *somas*, while the blue line would be the border of the circular culture with diameter ϕ. The values of the parameters implemented to create the networks are: $N = 2,000$ neurons, $\phi = 3$ mm, $\phi_d = 15$ μm, $\mu_d = 300$ μm, $\sigma_d = 40$ μm, $\sigma_\ell = 800$ μm, $\Delta\ell = 10$ μm, $\sigma_\theta = 0.1$ rad. (For interpretation of the references to color in this figure legend, the reader is referred to the web version of this article.)

the end of the soma, with its orientation set randomly; and the following segments are placed at the end of the previous one, with their orientation θ given by a Gaussian distribution centered at the previous segment and a standard deviation σ_θ, as

$$p(\theta_i) = \frac{1}{\sqrt{2\pi\sigma_\theta^2}} \exp\left(-\frac{(\theta_i - \theta_{i-1})^2}{2\sigma_\theta^2}\right). \tag{16}$$

Considering the former neuronal description, a neuronal network with N neurons is constructed following these steps:

(*i*) The N soma centers are laid down on a circular area with open boundary conditions according to a spatial probability distribution and no overlap between neurons. In order to mimic experimental observations [7,38], this spatial probability distribution is chosen by linear summation of n_G Gaussian functions with random centers and variance σ_G^2. This allows a control for the degree of aggregation in the network, measured through the Gini coefficient [38], and termed Λ. In this way, the aggregation of the network Λ increases as n_G decreases and *viceversa*, as shown in Fig. 5(b).

(*ii*) Each neuron is then set with its dendritic tree and axon, placing one segment after another until the total axonal length is reached.

(*iii*) Finally, a connection $i \to j$ between neurons i and j is established with probability α whenever the axon of neuron i intersects the dendritic tree of neuron j, as sketched in Fig. 5(a).

We note that the connectivity probability α is independent of the overlapping length between the axon and the dendritic tree and therefore $\langle k\rangle \propto \alpha$. Additionally, it can be numerically derived that $\sigma_k^2 \approx \frac{1}{3}\langle k\rangle$, leading to the following approximation for the second moment of the degree distribution of the neuronal network:

$$\langle k^2\rangle \approx \langle k\rangle\left(\langle k\rangle + \frac{1}{3}\right). \tag{17}$$

The topological properties of the networks created following the rules described above are determined by the chosen values of α (and thus $\langle k\rangle$), ℓ_{MAX} and Λ. Moreover, by substituting Eq. (17) in Eq. (12), we can obtain the same scaling $g_C \sim \langle k\rangle^{-1}$ observed for ER networks. This similarity can be understood taking into account that the degree distribution of our biologically-realistic networks is similar to that of a network built through the ER model, although wider and with longer tails [8].

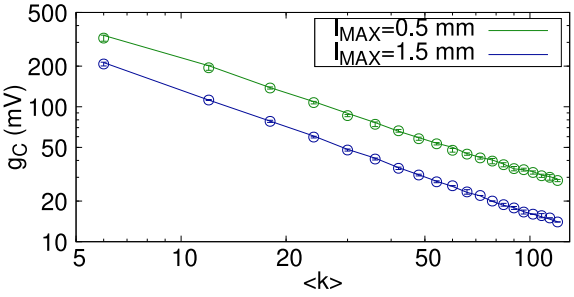

Fig. 6. Dependence of g_C on $\langle k\rangle$ in spatial networks of size $N = 2000$ nodes. The plots show a comparison between the numerical solutions of spatial networks (dots) and the theoretical prediction $g_C \sim \langle k\rangle^{-1}$ (lines) for two different maximum axonal lengths, $\ell_{MAX} = 0.5$ mm and 1.5 mm. The values of g_C are averaged over $n = 25$ network realizations for the same $\langle k\rangle$. The theoretical predictions have been evaluated by computing the average maximum eigenvalue of the networks and introducing it in Eq. (12) with $\gamma = 5.5$.

As in the previous section, we now compare the numerical values obtained for g_C with their theoretical predictions. To this aim, we fix the degree of aggregation to $\Lambda \approx 0.6$, which is a typical value of *in vitro* neuronal networks [38], and considered two contrasting axonal lengths, $\ell_{MAX} = 0.5$ and 1.5 mm. Then, we generated neuronal networks for a wide range of $\langle k\rangle$ values. The comparison is shown in Fig. 6. The numerically obtained values keep the $g_C \sim \langle k\rangle^{-1}$ scaling and agree fairly well with the predictions of Eq. (12) for the ER model. As stated before, we argue that this similarity is due to the similar degree distributions of the spatial and ER models,

Finally, given the similar values of g_C provided by the numerical simulations and Eq. (12), we next explore in more detail the dependence of g_C on different network parameters through just Eq. (12). Thus, we studied the dependency of g_C on $\langle k\rangle$, Λ and ℓ_{MAX} when either ℓ_{MAX} was fixed to 1.5 mm (Fig. 7(a)) or when Λ was fixed to 0.6 (Fig. 7(b)). In general, we observe that g_C decreases as $\langle k\rangle$, Λ and l_{MAX} grow. This is due to the fact that an increase in $\langle k\rangle$ or ℓ_{MAX} leads a higher number of connections from a given neuron to its neighbors. Thus, the effective amount of external inputs delivered to a small region of the network could be sufficient to activate it, even if the individual strength of each synaptic pulse is relatively low. For the case

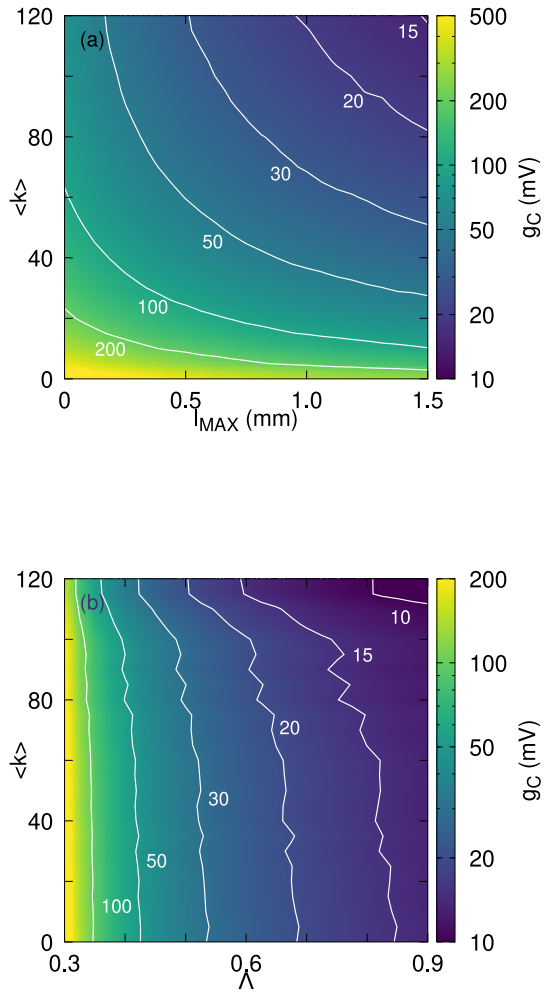

Fig. 7. Color map of the critical coupling g_C as a function of the average degree of the neuronal network, $\langle k \rangle$, the maximum axonal lengths $\ell_{MAX} = 1.5$, and the aggregation coefficient, Λ. In panel (a) we fix $\Lambda \approx 0.6$ and show $g_C(\ell_{MAX}, \langle k \rangle)$, while in panel (b) we fix $\ell_{MAX} = 1.5$ mm and show $g_C(\Lambda, \langle k \rangle)$. In both panels the white curves correspond to contour lines for a fixed value of g_C. In general, g_C increases as $\langle k \rangle$, Λ and ℓ_{MAX} decrease. For both these panels a value of $\gamma = 5.5$ was used.

of increasing Λ the same argument holds, since strongly aggregated neurons shape by themselves high connectivity clusters.

6. Discussion

In this work, we aimed to uncover the laws governing the activation of neuronal networks by studying the role of connectivity, long-range connections, and degree of aggregation. Our approach involved describing network dynamics using the Izhikevich model and deriving the Master Stability Function (MSF) of the system around the stable fixed point corresponding to an inactive neuron. This way, it is possible to eventually derive the maximum value of the coupling between neurons, g_C, that allows for the stability of the quiescent state or, in other words, the minimum coupling necessary for the network to activate, depending only on the parameters of the dynamical model and the topological properties of the layout of connections between neurons.

Our results show that the MSF for a simple version of the Izhikevich model, used to estimate g_C in Eq. (12), accurately predicts the numerical estimated critical coupling obtained when implementing a more realistic version of both the Izhikevich dynamical model and the architecture of the neuronal network. This demonstrates the ability of the proposed formalism to capture the interplay between topology and dynamics in both simple (ER and BA models) and biologically realistic constructions, provided that the connectivity is large enough for the largest component of the network to be fully formed. Based on these results, we have used Eq. (12) to explore the behavior of the neuronal networks for different structural parameters. Specifically, we have studied the dynamics of a realistic, biologically-inspired model for a range of values in connectivity, axonal lengths, and aggregation. Our results show that lower values of synaptic strength are needed to have an active network as the connectivity, connection distance, and degree of aggregation increase.

In conclusion, our work provides insights into the principles governing the activation of neuronal networks and highlights the importance of considering both intrinsic parameters of the model and topological properties of the layout of connections in the network. The proposed formalism, based on the MSF for the Izhikevich model, allows for accurate predictions of critical coupling in both synthetic and realistic structures, making it a useful tool for exploring the behavior of experimental neuronal cultures under different structural conditions. In addition, our results pave the way to the understanding of more complex interaction structures [17,39] as well as to the design of architectures with potentially new dynamical behaviors.

CRediT authorship contribution statement

Sergio Faci-Lázaro: Investigation, Formal analysis, Writing – original draft. **Jordi Soriano:** Conceptualization, Investigation, Writing – original draft. **Juan José Mazo:** Supervision, Conceptualization, Investigation, Writing – original draft. **Jesús Gómez-Gardeñes:** Supervision, Conceptualization, Investigation, Writing – original draft.

Declaration of competing interest

The authors declare that they have no known competing financial interests or personal relationships that could have appeared to influence the work reported in this paper.

Data availability

No data was used for the research described in the article.

Acknowledgments

S.F.-L., J.J.M and J.G.-G. acknowledge financial support from the Departamento de Industria e Innovación del Gobierno de Aragón *y* Fondo Social Europeo (FENOL group grant E36-23R) and from grant PID2020-113582GB-I00 funded by MCIN/AEI/10.13039/50110 0011033. J.S. acknoweledges financial support from the Generalitat de Catalunya, Spain, grant 2021-SGR-00450, and Ministerio de Ciencia e Innovación (Spain), grant PID2019-108842GB-C21.

References

[1] Bullmore E, Sporns O. Complex brain networks: Graph theoretical analysis of structural and functional systems. Nat Rev Neurosci 2009;10(3):186–98.
[2] Chialvo DR. Emergent complex neural dynamics. Nat Phys 2010;6(10):744–50.
[3] Levina A, Herrmann JM, Geisel T. Dynamical synapses causing self-organized criticality in neural networks. Nat Phys 2007;3(12):857–60.
[4] Soriano J, Rodríguez Martínez M, Tlusty T, Moses E. Development of input connections in neural cultures. Proc Natl Acad Sci 2008;105(37):13758–63.
[5] Feinerman O, Rotem A, Moses E. Reliable neuronal logic devices from patterned hippocampal cultures. Nat Phys 2008;4(12):967–73.
[6] Cohen O, Keselman A, Moses E, Martínez MR, Soriano J, Tlusty T. Quorum percolation in living neural networks. Europhys Lett 2010;89(1):18008.
[7] Orlandi JG, Soriano J, Alvarez-Lacalle E, Teller S, Casademunt J. Noise focusing and the emergence of coherent activity in neuronal cultures. Nat Phys 2013;9(9):582–90.
[8] Faci-Lázaro S, Soriano J, Gómez-Gardeñes J. Impact of targeted attack on the spontaneous activity in spatial and biologically-inspired neuronal networks. Chaos 2019;29(8):083126.

[9] Faci-Lázaro S, Lor T, Ródenas G, Mazo JJ, Soriano J, et al. Dynamical robustness of collective neuronal activity upon targeted damage in interdependent networks. Eur. Phys. J. Spec. Top. 2022;231(3):195–201. http://dx.doi.org/10.1140/epjs/s11734-021-00411-7.
[10] Maeda E, Robinson H, Kawana A. The mechanisms of generation and propagation of synchronized bursting in developing networks of cortical neurons. J Neurosci 1995;15(10):6834–45.
[11] Opitz T, De Lima AD, Voigt T. Spontaneous development of synchronous oscillatory activity during maturation of cortical networks in vitro. J Neurophysiol 2002;88(5):2196–206.
[12] Marom S, Shahaf G. Development, learning and memory in large random networks of cortical neurons: Lessons beyond anatomy. Q Rev Biophys 2002;35(1):63–87.
[13] Wagenaar DA, Pine J, Potter SM. An extremely rich repertoire of bursting patterns during the development of cortical cultures. BMC Neurosci 2006;7(1):1–18.
[14] Cohen E, Ivenshitz M, Amor-Baroukh V, Greenberger V, Segal M. Determinants of spontaneous activity in networks of cultured hippocampus. Brain Res 2008;1235:21–30.
[15] Ham MI, Bettencourt LM, McDaniel FD, Gross GW. Spontaneous coordinated activity in cultured networks: Analysis of multiple ignition sites, primary circuits, and burst phase delay distributions. J Comput Neurosci 2008;24(3):346–57.
[16] Hernández-Navarro L, Faci-Lázaro S, Orlandi JG, Feudel U, Gómez-Gardeñes J, Soriano J. Noise-driven amplification mechanisms governing the emergence of coherent extreme events in excitable systems. Phys. Rev. Res. 2021;3(2):023133.
[17] Yamamoto H, Moriya S, Ide K, Hayakawa T, Akima H, Sato S, et al. Impact of modular organization on dynamical richness in cortical networks. Sci Adv 2018;4(11):eaau4914.
[18] Hernández-Navarro L, Orlandi JG, Cerruti B, Vives E, Soriano J. Dominance of metric correlations in two-dimensional neuronal cultures described through a random field ising model. Phys Rev Lett 2017;118(20):208101.
[19] FitzHugh R. Impulses and physiological states in theoretical models of nerve membrane. Biophys J 1961;1(6):445–66.
[20] Nagumo J, Arimoto S, Yoshizawa S. An active pulse transmission line simulating nerve axon. Proc. IRE 1962;50(10):2061–70.
[21] Izhikevich EM. Simple model of spiking neurons. IEEE Trans Neural Netw 2003;14(6):1569–72.
[22] Izhikevich EM. Dynamical systems in neuroscience. MIT Press; 2007.
[23] Alvarez-Lacalle E, Moses E. Slow and fast pulses in 1-D cultures of excitatory neurons. J Comput Neurosci 2009;26(3):475–93.
[24] Pecora LM, Carroll TL. Master stability functions for synchronized coupled systems. Phys Rev Lett 1998;80(10):2109.
[25] Newman M. Networks: An introduction. Oxford University Press; 2010.
[26] Porter MA, Gleeson JP. Dynamical systems on networks. Front Appl Dyn Syst: Rev Tutor 2016;4.
[27] Gade PM, Cerdeira HA, Ramaswamy R. Coupled maps on trees. Phys Rev E 1995;52:2478–85. http://dx.doi.org/10.1103/PhysRevE.52.2478, URL https://link.aps.org/doi/10.1103/PhysRevE.52.2478.
[28] Gade PM. Synchronization of oscillators with random nonlocal connectivity. Phys Rev E 1996;54:64–70. http://dx.doi.org/10.1103/PhysRevE.54.64, URL https://link.aps.org/doi/10.1103/PhysRevE.54.64.
[29] Arenas A, Díaz-Guilera A, Kurths J, Moreno Y, Zhou C. Synchronization in complex networks. Phys Rep 2008;469(3):93–153.
[30] Izhikevich EM. Which model to use for cortical spiking neurons? IEEE Trans Neural Netw 2004;15(5):1063–70.
[31] Cohen D, Segal M. Network bursts in hippocampal microcultures are terminated by exhaustion of vesicle pools. J Neurophysiol 2011;106(5):2314–21.
[32] Cohen D, Segal M. Homeostatic presynaptic suppression of neuronal network bursts. J Neurophysiol 2009;101(4):2077–88.
[33] Chung F, Lu L, Vu V. The spectra of random graphs with given expected degrees. Internet Math 2004;1(3):257–75.
[34] Restrepo JG, Ott E, Hunt BR. Approximating the largest eigenvalue of network adjacency matrices. Phys Rev E 2007;76(5):056119.
[35] Erdös P, Rényi A. On random graphs i. Publ Math 1959;6:290–7.
[36] Erdös P, Rényi A, et al. On the evolution of random graphs. Publ Math Inst Hung Acad Sci 1960;5(1):17–60.
[37] Barabási A-L, Albert R. Emergence of scaling in random networks. Science 1999;286(5439):509–12.
[38] Tibau E, Ludl A-A, Ruediger S, Orlandi JG, Soriano J. Neuronal spatial arrangement shapes effective connectivity traits of in vitro cortical networks. IEEE Trans Netw Sci Eng 2020;7(1):435–48.
[39] Montalà-Flaquer M, López-León CF, Tornero D, Houben AM, Fardet T, Monceau P, et al. Rich dynamics and functional organization on topographically designed neuronal networks in vitro. Iscience 2022;25(12):105680.